# Formation of annealing twins during recrystallization and grain growth in 304L austenitic stainless steel

Y.JIN[1, a], M.BERNACKI[1], G.S.ROHRER[2], A.D.ROLLETT[2], B.LIN[2], N.BOZZOLO[1]

[1]CEMEF, Rue Claude Daunesse, Sophia Antipolis, 06904, France

[2]Carnegie Mellon University, 5000 Forbes Avenue, Pittsburgh, 15213, USA

[a]yuan.jin@mines-paristech.fr

**Keywords:** Annealing twins, recrystallization, grain growth, *in situ* annealing, EBSD.

**Abstract.** Understanding of the mechanisms of annealing twin formation is fundamental for grain boundary engineering. In this work, the formation of annealing twins in a 304L austenitic stainless steel is examined in relation to the thermo-mechanical history. The behavior of annealing twins of various morphologies is analyzed using an in-situ annealing device and EBSD. The results confirm that there is a synergistic effect of prior strain level on annealing twin density generated during recrystallization. The higher the prior strain level, the higher the velocity of grain boundary migration and the higher the annealing twin density in the recrystallized grains. This effect decreases as the recrystallization fraction increases. The existing mathematical models (Pande's model and Gleiter's model), which were established to predict annealing twin density in the grain growth regime, can not predict this phenomenon.



## 1. Introduction

In 1926, Carpenter and Tamura [1] were the first to observe the formation of annealing twins. Since then, annealing twins have been observed in a variety of deformed and subsequently annealed F.C.C. materials. A "twin" refers to a grain that has one or two twin boundaries with a larger grain in which it is embedded. For the F.C.C. crystal structure, the twin boundary misorientation can be obtained by rotating the orientation of the parent grain 60° about<111>. For a coherent twin boundary, the boundary plane is parallel to {111} plan while the boundary plane differs from {111} plane for an incoherent twin boundary. Being one of the most important kinds of special boundaries, annealing twin boundaries affect many properties like anti-corrosion and anti-fatigue in a large variety of materials, including such technologically important material as superalloys [2]. Today, eighty years after the discovery of annealing twins, metallurgists still do not have a clear understanding of their formation. The growth accident theory, which suggests that a coherent twin boundary forms at a migrating grain boundary due to a stacking error, is supported by a majority of recent experimental results [3-5]. In the growth accident theory, the migration distance and migration velocity of grain boundary are two key positive factors to annealing twin generation. However, the only two mathematical models based on this theory [6,7], which were established to predict annealing twin density in the grain growth regime, are not capable of predicting annealing twin density in the recrystallization regime. The aim of the present work is to extract some regular patterns of annealing twin formation during recrystallization especially the relationship between the stored energy level and the annealing twin density by analysing the experimental results from a 304L austenitic stainless steel.

## 2. Experimental details

**2.1 Material and thermo-mechanical treatments.** Austenitic stainless steels, which do not undergo discernible phase transformation during their hot working over a wide temperature range, are ideal model alloys to investigate recrystallization. 304L austenitic stainless steel has a low stacking fault energy ($\approx 0.02 \mathrm{Jm}^{-2}$) and so annealing twins are generated easily [8]. That is why this alloy is also favorable for annealing twin formation observation. The melting temperature of 304L is 1400°C. The recrystallization phenomena of 304L was analysed in detail in the PhD work of K. HUANG [9]. The chemical composition (weight percentage) of the material is given in Table 1. In

the following, two 304L samples are analyzed. Both samples have been submitted to a hot torsion test, at the same strain rate but with a different strain level: ε=0.3 (sample 1) and 1.5 (sample 2). As the average grain size in sample 1 is apparently bigger than in sample 2, sample 2 was very likely dynamically recrystallized during the hot deformation. However, according to the experimental results that will be shown in the next section, sample 2 that was deformed with higher strain level has higher stored energy level.

*Chemical composition of 304L*

| C | Mn | Si | P | S | Cr | Ni | N |
|---|---|---|---|---|---|---|---|
| <0.03 | <2.00 | <0.75 | <0.045 | 0.03 | 8.0~12.0 | 8.0~112.0 | <0.10 |

Table 1, Chemical composition of 304L

After thermo-mechanical treatment, samples were water quenched to fix as much as possible the microstructure. After the quenching, the samples were annealed at 1000°C inside a SEM chamber using an *in situ* annealing device [10]. *In situ* observations were performed sequentially during the anneal using an Electron Backscattered Diffraction (EBSD) system. Several scans were collected during the heat treatment, and the EBSD acquisitions were analyzed with the OIM software.

**2.2 Quantitative analysis of the microstructures.** Annealing twins are quantified by their density, which is defined as the number of intercepts of annealing twin boundaries per unit length [7]. Both coherent and incoherent twins are taken into account. In the OIM software, annealing twins are defined by a misorientation by 60° along the axis <111> with a tolerance of 8.66° according to the Brandon criterion [11].

In the present work, the annealing twin density is determined only in the recrystallized grains. The recrystallized grains are extracted from the EBSD maps by applying a criterion that the GOS (Grain Orientation Spread) value must be smaller than 1° as illustrated by Fig. 1, The annealing twin density is obtained by using Eq. 1[12], where $L_{tb}$ is the total length of annealing twin boundaries and $S_{rg}$ is the surface area of recrystallized grains,

$$\text{Twin Density} = \frac{L_{tb}}{S_{rg}} \times \frac{2}{\pi} \quad . \tag{1}$$

The average grain size is evaluated in the OIM software with a minimum that equals 5° and twins are ignored in the evaluation. The average grain boundary migration velocity is estimated as the change of average grain size of recrystallized grains per unit time. More precisely, the average migration velocity equals the ratio between the change of average grain size and the time increment between two successive EBSD acquisitions.

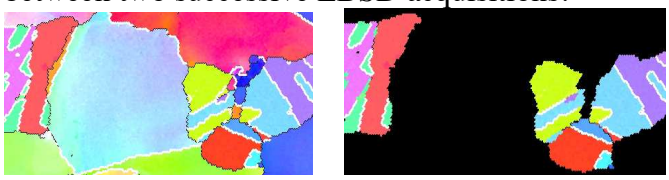

(a) All grains (b) Recrystallized grains

Fig .1, Sample 1 microstructure, (a): EBSD map obtained from Sample 1 after a short annealing; and (b) Recrystallized grains detected using GOS<1°; thick, white lines denote Σ3 boundaries.

## 3. Experimental results

**3.1 Statistical analyses.** In Fig .2, the evolutions of annealing twin density, recrystallization fraction, and average grain boundary migration velocity of the two samples are shown. As the average grain boundary migration velocity is higher in sample 2 than in sample 1 and the average grain size of recrystallized grains in sample 2 is smaller than in sample 1, sample 2 has certainly a higher stored energy level than sample 1. Sample 2, which was more deformed than sample 1, has not only slightly bigger maximum value of twin density but also higher twin density for a given average grain size (≈30$\mu$m) compared with sample 1. In addition, in both samples the twin density increases as the recrystallization fraction increases at the beginning of the recrystallization regime and the maximum value of annealing twin density corresponds to the maximum value of grain boundary migration velocity. Both the stored energy level and the average grain size influence positively the average grain boundary migration velocity in the recrystallization regime. The higher

stored energy level of sample 2 has a synergistic influence on annealing twin density via its accelerating effect on grain boundary migration. This observation is consistent with the Growth Accident Theory [13]. Finally since the remnant stored energy level decreases continuously during the recrystallization regime, the positive effect of the initial stored energy level on annealing twin density mitigates as well.

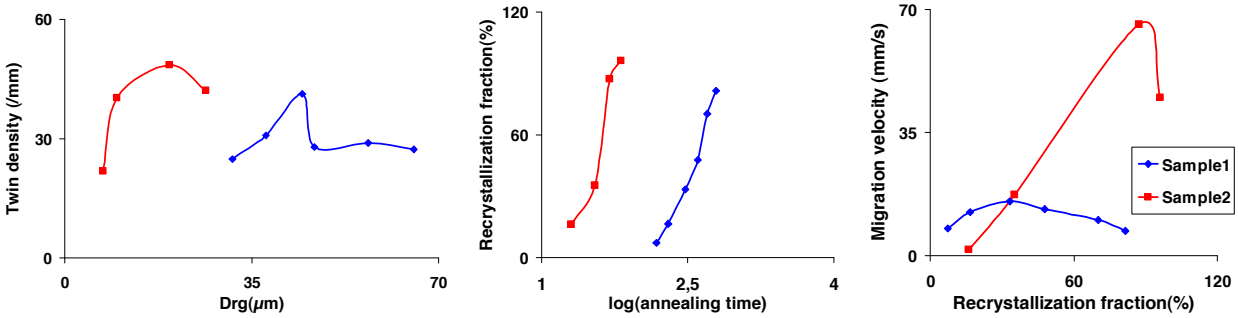


(a) (b) (c)

Fig .2, (a): Evolution of annealing twin density vs average recrystallized grain size; (b): evolution of recrystallization fraction vs annealing time at 1000°C; and (c): Evolution of average grain boundary migration velocity as a function of recrystallization fraction.

**3.2 Topological analyses.**

**3.2.1 Evolution of annealing twins with different morphologies.** *In situ* studies offer an opportunity to classify and quantify annealing twins on a topological basis. Annealing twins in F.C.C. alloys exhibit four morphologies labelled A, B, C, D in Fig .3 [14]. This classification is based on 2D sections. Real annealing twin morphologies could be observed only by performing 3D characterization [15, 16]. The growth accident theory, which is supported by many experimental evidences, is considered as the theoretical basis of the annealing twin formation mechanism. However, there is no specific atomistic model based on this theory that could explain the formation mechanisms of all these four kinds of annealing twins [6, 7, 13, 14]. *In situ* observations offer an opportunity to study the generation process of the twins with different morphologies. In order to determine if the different annealing twins are formed with equal probability and their preferential formation location, the newly generated twins with these four morphologies in each *in situ* scan are counted separately. For statistical analysis, only the recrystallized grains are taken into account. In addition, to analyze the evolution of annealing twins during the growth of grains, the newly generated twins are counted only in the grains that can be identified in the previous EBSD scan.

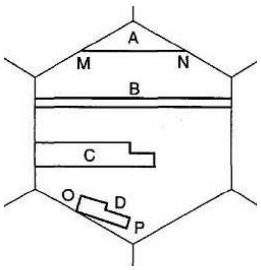


Fig .3, Four morphologies of annealing twins in 2D [14]

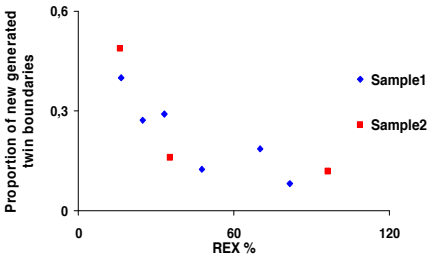


Fig .4, Proportion of newly generated twins

The evolution of the proportion of newly formed annealing twins including all the four types in sample 1 and sample 2 among all the annealing twins that can be identified is shown in Fig .4. In both samples, this proportion is higher at the beginning than at the end of the recrystallization regime. This phenomenon is consistent with the conclusion of the statistic analysis. As the average grain boundary velocity is much lower at the end than at the beginning of the recrystallization regime and as the annealing twin formation probability increases with the migration velocity according to the growth accident theory [6, 7, 13, 14], the fact that there are fewer newly generated annealing twins at the end of the recrystallization regime is logical. In addition, when approaching the grain growth regime (Rex%>80%), as the proportion of newly generated twins is around 10%, the evolution of annealing twin density is mainly determined by the propagation, the interaction or the disappearance of the existing twins. However, both of the existing predictive mathematical

models (Gleiter's model [6] and Pande's model [7]) were established to simulate the annealing twin generation but not the propagation or annihilation.

**3.2.2 Topological evolution of annealing twins.** As already mentioned, in the grain growth regime, the change of the annealing twin density is mostly determined by the propagation, the interaction or the disappearance of the existing twins, that is why it is crucial to study the morphological evolution of annealing twins. Since the grain growth regimes in the two analyzed samples are short, two successive *in situ* EBSD scans of another sample that underwent similar thermo-mechanical treatment but has relatively more information of the grain growth regime are chosen to analyze topological evolutions of annealing twins, shown in Fig .5.

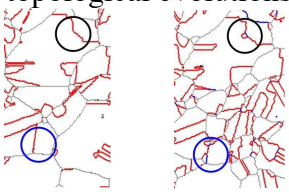

Fig .5, Thick, red lines denote Σ3 boundaries; thick blue lines denote Σ9 boundaries; thin black lines represent normal high misorientation boundaries (misorientation > 5°)

In Fig .5, two representative annealing twin topological changes are marked by black and blue circles. For the black circle marked change, the twin boundaries migrated due to the capillarity force, while a Σ9 boundary merged into a Σ3 boundary. The decrease of the total free energy is the driving force of this evolution. Three different transformations contribute to this reduction: decrease of the total boundary length, transformation from Σ9 boundary to Σ3 boundary, and disappearance of the two triple junctions. For the blue circle marked change, an incoherent twin boundary merged into a coherent twin boundary while the interface, which is a Σ9 boundary, between the incoherent and coherent parts faded away. Since both Σ9 boundary and incoherent twin boundary have greater interfacial energy than coherent twin boundary [17], this transformation is also energetically favorable. To summarize, Σ3 and Σ9 boundaries evolve to minimize the total interfacial energy.

**4. Conclusion**

The annealing twins are generated mostly during the recrystallization regime. In the grain growth regime, the evolution of annealing twin density is mainly determined by the propagation, the interaction or the disappearance of the existing twins. A higher stored energy level favors the formation of annealing twins, but mainly at the beginning of the recrystallization regime. In the grain growth regime, incoherent twin boundaries are mobile, which allows the Σ3 and Σ9 boundaries to evolve to minimize the total interfacial energy.

**5. Acknowledgements.** The authors are very grateful to Dr K. Huang and S. Jacomet for providing the data analyzed in this paper. B. Lin and A.D. Rollett are also grateful for support from NSF.

**References**

[1] H.C.H. Carpenter and S.Tamura. Proceedings of the Royal Society A, 113(763): 28-43,1926
[2] M.A. Imam B.B. Rath and C.S. Pande. Mater. Phys. Mech., 2000
[3] J.R. Cahoon, Q. Li and N.L. Richards. Materials Science and Engineering: A,526:56-61,2009
[4] Q. Li, J.R. Cahoon and N.L. Richards, Scripta Materialia, 55(22): 1155-1158, 2006
[5] K.H. Song, Y.B. Chun and S.K. Hwang. Materials Science and Engineering: A,629-636, 2007
[6] H. Gleiter. 17(12):1421-1428, 1969
[7] C.S. Pande. Metallurgical Transactions A, 21A: 2891-2896, 1990
[8] E.M. Lehockey, G. Palumbo and P.Lin. JOM, 50(2):40-43 1998
[9] K. Huang. PhD thesis, Mines ParisTech, 2011
[10]N. Bozzolo, S. Jacomet and R.E. Logé. Materials Characterization, 70: 28-32, 2012
[11]D.G. Brandon. Acta Metall., 14(11):1479-1484, 1966
[12]E.E. Underwood. Addison-Wesley publishing company, 1970
[13]M. Meyers. Interface Migration and Control of Microstructure, 17-21, 1984
[14]M.A. Imam, S. Mahajan, C.S. Pande and B.B.Rath. Acta Metallurgica, 2633-2638, 1997
[15]C.M. Hefferan, J. Lind, S.F. Li and U. Lienert. Acta Materialia, 1: 1-17,2012
[16]J. Li S.J. Dillon and G.S. Rohrer. Acta Materialia, 57(14):4304-4311, 2009
[17]D.L. Olmsted, S.M. Foiles and E.A. Holm. Acta Materialia, 57(13): 3694-3703, 2009